European Conference on Computational Fluid Dynamics
ECCOMAS CFD 2006
P. Wesseling, E. Oñate and J. Périaux (Eds)

A POSTERIORI ERROR ANALYSIS FOR STOCHASTIC FINITE ELEMENT SOLUTIONS OF FLUID FLOWS WITH PARAMETRIC UNCERTAINTIES

Lionel Mathelin† and Olivier P. Le Maître*

†Laboratoire d'Informatique pour la Mécanique et les Sciences de l'Ingénieur
LIMSI-CNRS, BP 133, 91 403 Orsay cedex, France
e-mail: mathelin@limsi.fr
*Université d'Evry Val d'Essonne, LMEE
4, rue du Pelvoux, CE 1455, 91 020 Evry cedex, France
e-mail: olm@iup.univ-evry.fr

Key words: Stochastic finite elements, error analysis, Polynomial Chaos, Uncertainty quantification.

Abstract. *Accounting for uncertainty in numerical simulations is a growing concern and a great deal of methods have recently been developed, such as the Polynomial Chaos which basically consists in a spectral approximation of the surface response of the solution by stochastic finite elements. However, criteria for refinement of the spectral space have so far been rather heuristic. In this paper, a more rigorous approach is proposed based on an a posteriori error analysis combined with a hp-Polynomial Chaos formulation. This error analysis provides a good estimate of the local error and can thus trigger refinement both in the spectral order (p-refinement) or/and in the element-support (h-refinement).*

This technique is applied to the Burgers equation considered with an uncertain viscosity depending on two independent random variables. It is shown that the proposed method allows to effectively refine the numerical approximation of the solution only where needed and leads to a very limited number of variables while retaining a good accuracy in the solution.

1 INTRODUCTION

Due to the impressive level of performance of the recent computers and because numerical algorithms have earned efficiency and speed, one is willing to enhance the physics in the numerical simulations to make the computations closer to the full complexity of the real life. This is done by taking into account additional physical phenomena, of second-order and thus neglected before, to improve the accuracy of the modelization. In that perspective, one has to address issues little considered before such as uncertainty intrinsically embedded in the problem physical parameters, initial or boundary conditions, poorly known physical properties, etc... The numerical simulations are now expected to provide

confidence bounds on the results considering the uncertainty in the input parameters. In some cases, and in fact in most, the number of independent random variables affecting the output of the simulation can be large and the computation of the deterministic solution may be expensive in terms of CPU time, preventing the use of brute-force methods and requiring a careful treatment to keep the problem tractable. It is thus necessary to limit to a minimum the number of calculations required to reach a certain level of accuracy.

The question is then how to quantify this uncertainty in the solution ? Several well known techniques may be used to answer this question including, among others, the Monte-Carlo method and its accelerated variants (Latin Hypercube Sampling, Importance Sampling, Simulated Annealing, etc.) or the sensitivity analysis based on the first order approximation of the problem variables dependence on the uncertainty parameters. While the sensitivity method is limited to small variance only, the Monte-Carlo technique is very general and its simplicity makes it a popular approach. However its convergence error scales as $1/\sqrt{n}$, n being the number of samples, achieving a low convergence rate and preventing its use for most realistic problems which often involve a large amount of CPU time for a single sample (realization). An alternative technique is the so-called Polynomial Chaos[1] (PC) which basically consists in expanding all random variables of the problem in a spectral decomposition under the form of a converging series. This method has been successfully applied to a great deal of systems and configurations (see for instance[2–7]) but suffers from the same limitations as all spectral-based methods. In particular, it can not handle very steep or discontinuous quantities as it would require a very high spectral order and would lead both to poorly conditioned and untractable problems.

In this framework, the goal is then to minimize the number of terms of the series while still achieving a good representation of the surface response over the entire stochastic space. Le Maître *et al.* (2004)[8] have decomposed the stochastic space in several subdomains in which the problem is solved independently from the other subproblems. Within the subdomains, a low order polynomial expansion is used to represent the solution. A criterion based on the ratio between the directional and the global energy (variance) of the current decomposition in PC series triggers a h-refinement based on a preset threshold criterion. Similarly, Wan & Karniadakis (2005)[9] uses a hp-spectral expansion in the stochastic space. The refinement is also based on heuristic arguments involving the relative contribution of the last order of the polynomial chaos expansion solely to the local variance. A dimension i is further h-refined if the contribution to the variance of the last term involved from direction i is above a preset threshold value. Although those schemes are giving a significant improvement over the regular spectral polynomial chaos methods in terms of robustness and computational efficiency, they still lack rigorous criteria for triggering the refinement. In particular, the choice of the direction to refine is left to loose criteria.

In this paper, a test problem of uncertainty quantification is considered using a stochastic spectral element formulation. A refinement procedure of the discrete solution is derived in the spirit of an a posteriori error analysis commonly used in the finite element com-

munity. It relies on well established grounds and allows to derive a rigorous estimation of the error resulting from the solution of the discretized problem solved in a variational form.

The resolution of a problem involving uncertain quantities is succinctly presented in section 2 in variational formulation. In section 3, fundamentals of the a posteriori error analysis is presented, together with the primal and dual problems formulation and an estimate of the error is finally derived. The discretization and refinement techniques are provided in section 4. In particular, the discretization used in the spatial and stochastic subspaces is provided and the refinement procedure is explicited. An example of application of the a posteriori analysis to the uncertain Burgers equation and discussion of the results is proposed in section 5.

2 VARIATIONAL FORMULATION OF UNCERTAIN FLOWS

Let us consider the problem of the resolution of a given steady flow model (Navier-Stokes, Euler, Burgers, ...) in a domain $\Omega_x \subset \mathbb{R}^m$. We assume that the model involves a finite number of uncertain parameters denoted by the vector d, for instance boundary condition value, the fluid viscosity... Let us denote the model solution u; a variational formulation of the problem is

$$\begin{cases} A(u;\varphi|d) = F(\varphi|d) & \forall \varphi \in V_x \\ u = u_{\partial\Omega_x}(d) & \text{on } \partial\Omega_x \end{cases} \tag{1}$$

where V_x is a suitable Hilbert space of Ω_x, A a differentiable semi-linear form and F a linear functional. In Eq. (1), we have made explicit the dependence of the model on the vector of uncertain parameters d. Clearly, the solution u is also a function of d.

Since d is uncertain, it is suitable to consider it as a random vector defined on an abstract probability space $(\mathcal{A}, \sigma, dP)$. In this context, the solution of the model is also random. In the following, we adopt the convention consisting in using uppercase letters to denote random quantities. Thus, the random solution U and the random vector D are dependent stochastic quantities defined on the same probability space $(\mathcal{A}, \sigma, dP)$, the dependency being fixed by the model. Uncertainty propagation consists in the inference of the probability law of U, given the probability law of D and the model.

To this end, the Polynomial Chaos expansions and their recent extensions have proved their effectiveness. All of these techniques assume that D can be expressed in terms of a finite number of independent identically distributed real valued random variables ξ_i defined on $(\mathcal{A}, \sigma, dP)$ with value in $S_\xi \subset \mathbb{R}$:

$$D = D(\xi), \quad \xi = \{\xi_1, \ldots, \xi_n\} \in (S_\xi)^n \equiv \Omega_\xi \subset \mathbb{R}^n, \tag{2}$$

where the equality stands in the mean square sense. The probability density of the ξ_i is denoted p such that

$$p_\xi(\xi) = \prod_{i=1}^{n} p(\xi_i).$$

Without loss of generality, we shall take in the following $S_\xi = [-1, 1]$, such that $p(\xi_i \in S_\xi) = 1/2$, $p_\xi(\xi \in \Omega_\xi) = (1/2)^n$. Note also that the developments given below can be easily extended to the situation where the ξ_i have different ranges and/or different distributions.

The model being deterministic, in the sense that for a given realization of D it possesses a unique solution, the stochastic solution can also be written as a functional of the random variables : $U = U(\xi)$. Consequently, we have to solve $\forall \omega \in \mathcal{A}$:

$$\left\{ \begin{array}{ll} A(U(\xi(\omega)); \varphi | D(\xi(\omega))) = F(\varphi | D(\xi(\omega))) & \forall \varphi \in V_x \\ U(\xi(\omega)) = u_{\partial\Omega_x}(D(\xi(\omega))) & \text{on } \partial\Omega_x \end{array} \right. \tag{3}$$

To efficiently solve this equation, the PC-type methods[2,4,7,8,10,11] rely on the construction of a suitable Hilbert space V_ξ to represent the dependence of the solution and parameters on the random variables ξ_i. This Hilbert space can be constructed on various basis functions (global polynomials, piece-wise polynomials, wavelets, ...), but they all lead to generic expansions of D and U as

$$D(\xi) = \sum_k d_k \Psi_k(\xi), \quad U_k(\xi) = \sum_k u_k \Psi_k(\xi). \tag{4}$$

where the $\Psi_k \ : \xi \in \Omega_\xi \mapsto \mathbb{R}$ are orthogonal random functionals spanning V_ξ and d_k, u_k are the deterministic coefficients of the parameters and solution. The orthogonally of the random functional Ψ_k is defined with regard to the probability measure of ξ :

$$\begin{aligned} \langle \Psi_k \Psi_l \rangle &= \int_{\mathcal{A}} \Psi_k(\xi(\omega)) \Psi_l(\xi(\omega)) dP(\omega) \\ &= \int_{\Omega_\xi} \Psi_k(\xi) \Psi_l(\xi) p_\xi(\xi) d\xi = \left\langle \Psi_k^2 \right\rangle \delta_{kl}. \end{aligned} \tag{5}$$

Finally, letting $V \equiv V_x \times V_\xi$, the variational formulation of the problem is

$$\left\{ \begin{array}{ll} A(U; \Phi | D) = F(\Phi | D) & \forall \Phi \in V, \\ U = U_{\partial\Omega_x}(D) & \text{on } \partial\Omega_x, \end{array} \right. \tag{6}$$

to be solved for $U \in V$.

3 DUAL-BASED A POSTERIORI ERROR ESTIMATE

3.1 Primal and dual problems

We adopt the convention that the functionals are linear with respect to arguments placed on the right-side of a semicolon.

For a finite dimensional subspace $V_h \subset V$, the discretized solution $U_h \in V_h$ is the Galerkin approximation defined as the solution of the discrete problem

$$\left\{ \begin{array}{ll} A(U_h; \Phi_h | D_h) = F(\Phi_h | D_h) & \forall \Phi_h \in V_h \\ U_h = U_{\partial\Omega_x}(D_h) & \text{on } \partial\Omega_x \end{array} \right. \tag{7}$$

We denote $\mathscr{J}$, a differentiable functional of the solution. For instance $\mathscr{J}$ can be a velocity component, the kinetic energy of the flow or the pressure fields. Clearly, $\mathscr{J}$ is a random quantity defined on $(\mathcal{A}, \sigma, dP)$, and in the spirit of Babuska & Rheinboldt (1978)[12] and Babuska & Miller (1987)[13] among others, one is interested in approximating $\mathscr{J}(U)$ as closely as possible by $\mathscr{J}(U_h)$ in some sense, *i.e.* to minimize the difference $\mathscr{J}(U) - \mathscr{J}(U_h)$. For instance, one may try to minimize the second moment of the Euclidean distance $\|\mathscr{J}(U) - J(U_h)\|$ over the entire domain Ω_x with the corresponding error measure η :

$$\begin{aligned}
\eta^2 &= \int_{\Omega_x} E\left[\|\mathscr{J}(U) - \mathscr{J}(U_h)\|^2\right] dx \\
&= \int_{\Omega_x}\int_{\mathcal{A}} \|\mathscr{J}(U(x,\xi(\omega))) - \mathscr{J}(U_h(x,\xi(\omega)))\|^2 dP(\omega) dx \\
&= \int_{\Omega_x}\int_{\Omega_\xi} \|\mathscr{J}(U(x,\xi)) - J(U_h(x,\xi))\|^2 p_\xi(\xi) d\xi. \qquad (8)
\end{aligned}$$

Alternatively, the error may be defined over sub-domains (elements) of Ω_x and/or of Ω_ξ.

We now seek for expression of $\mathscr{J}(U) - \mathscr{J}(U_h)$. To this end, let us define $\mathscr{L}$, the Lagrangian of the continuous solution :

$$\mathscr{L}(U;Z) \equiv \mathscr{J}(U) + F(Z|D) - A(U;Z|D), \qquad (9)$$

where $Z \in V$ is the adjoint variable of the continuous problem. The adjoint variable Z is a Lagrange multiplier of the optimization problem for the minimization of $\mathscr{J}(U)$ under the constraint Eq. (3). This minimum corresponds formally to stationary points of the Lagrangian $\mathscr{L}$:

$$\frac{\partial \mathscr{L}}{\partial U} = \mathscr{J}'(U;\Phi') - A'(U;\Phi',Z|D) = 0, \quad \forall \Phi' \in V \qquad (10)$$

$$\frac{\partial \mathscr{L}}{\partial Z} = F(\Phi|D) - A(U;\Phi|D) = 0, \quad \forall \Phi \in V. \qquad (11)$$

Eq. (10) is the adjoint (or dual) problem, while Eq. (11) is the state (or primal) problem. Note that the derivatives are in the Gâteaux sense :

$$\begin{aligned}
J'(U;\Phi') &= \lim_{\epsilon\to 0} \frac{\mathscr{J}(U+\epsilon\Phi') - \mathscr{J}(U)}{\epsilon}, \\
A'(U;\Phi',Z|D) &= \lim_{\epsilon\to 0} \frac{A(U+\epsilon\Phi';Z|D) - A(U;Z|D)}{\epsilon}
\end{aligned}$$

The discrete counterpart of the dual and primal problems are in turn

$$\mathscr{J}'(U_h;\Phi'_h) - A'(U_h;\Phi'_h,Z_h|D_h) = 0, \quad \forall \Phi'_h \in V \qquad (12)$$

$$F(\Phi_h|D_h) - A(U_h;\Phi_h|D_h) = 0, \quad \forall \Phi_h \in V. \qquad (13)$$

Finally, we have

$$\begin{aligned}\mathscr{L}(U,Z)-\mathscr{L}(U_h,Z_h) &= \mathscr{J}(U)+F(Z)-A(U;Z)-\mathscr{J}(U_h)-F(Z_h)+A(U_h;Z_h)\\ &= \mathscr{J}(U)-\mathscr{J}(U_h), \end{aligned} \tag{14}$$

where the dependence of A and F on D has been dropped to simplify the notations. Eq. (14) shows that the difference in $\mathscr{J}$ of the continuous and discrete solutions is equal to the difference in their Lagrangians.

3.2 A posteriori error

To derive a more practical expression for the difference $\mathscr{J}(U)-\mathscr{J}(U_h)$ and following Becker & Rannacher (2001)[14], among others, let $K(\cdot)$ be a differentiable functional of u in a given functional space. The difference $K(u)-K(u_h)$ can be expressed as an integral between u and u_h of the derivative of K

$$K(u)-K(u_h)=\int_{u_h}^{u}K'(v)dv. \tag{15}$$

The integration path can be parameterized to obtain

$$\begin{aligned}K(u)-K(u_h) &= \int_0^1 K'(u_h+s(u-u_h))(u-u_h)ds\\ &= \int_0^1 K'(u_h+se_u;e_u)ds, \end{aligned} \tag{16}$$

where $e_u\equiv u-u_h$. Here, use was made again of the convention regarding the linearity of the functional forms with regard to the arguments on the right-side of the semi column. Assuming $K'(u)=0$ the right-hand side of Eq. (16) can be rewritten as

$$K(u)-K(u_h)=\int_0^1 K'(u_h+se_u;e_u)ds+\frac{1}{2}\left[K'(u_h;e_u)-K'(u_h;e_u)+K'(u;e_u)\right]. \tag{17}$$

Making use of the Galerkin orthogonality and the trapezoidal rule it comes

$$K(u)-K(u_h)=\frac{1}{2}K'(u_h;e_u)+\frac{1}{2}\int_0^1 K^{(3)}(u_h+s\,e_u;e_u^3)s(s-1)ds. \tag{18}$$

We now apply this relation to the difference of the Lagrangian of the continuous and discrete solutions. After some algebra we obtain

$$\mathscr{J}(U)-\mathscr{J}(U_h)=\frac{1}{2}\left[\rho(U_h,Z-\Phi_h')+\rho^*(Z_h,U-\Phi_h)\right]+\widetilde{R}, \tag{19}$$

with the residuals

$$\rho(U_h,\cdot) \equiv F(\cdot)-A(U_h;\cdot) \tag{20}$$

$$\rho^*(Z_h,\cdot) \equiv \mathscr{J}'(U_h,\cdot)-A'(U_h;\cdot,Z_h). \tag{21}$$

The remainder term $\widetilde{R}$ in Eq. (19) has for expression

$$\begin{aligned}\widetilde{R} &= \frac{1}{2}\int_0^1 \left[\mathscr{J}^{(3)}(U_h + sE_U; E_U^3) - A^{(3)}(U_h + sE_U; E_U^3, Z_h + sE_Z)\right. \\ &\quad \left. -3A''(U_h + sE_U; E_U^2 E_Z)\right] s(s-1)ds, \end{aligned} \tag{22}$$

with the errors terms defined as $E_U = U - U_h$ and $E_Z = Z - Z_h$. Thus $\widetilde{R}$ is cubic in the errors, suggesting that it can be neglected provided that the continuous and discrete solutions are sufficiently close. It is also seen that the residuals are functional of both the primal and dual continuous solutions U and Z, such that using Eq. (19) to estimate $\mathscr{J}(U) - \mathscr{J}(U_h)$ would required two surrogates of U and Z even if $\widetilde{R}$ is neglected. In fact, the expression can be further simplified to remove the contribution of U using an integration by part of $\widetilde{R}$; one obtains[14]

$$\rho^*(Z_h, U - \Phi_h) = \rho(U_h, Z - \Phi_h') + \Delta\rho, \tag{23}$$

where

$$\Delta\rho = \int_0^1 \left[A''(U_h + sE_U; E_U^2, Z_h + sE_Z) - \mathscr{J}''(U_h + sE_U; E_U^2)\right] ds. \tag{24}$$

Introducing this result in Eq. (19) we are lead to the final expression for the approximation error :

$$\mathscr{J}(U) - \mathscr{J}(U_h) = \rho(U_h, Z - \Phi_h') + R, \tag{25}$$

with

$$R = \int_0^1 \left[A''(U_h + sE_U; E_U^2, Z) - \mathscr{J}''(U_h + sE_U; E_U^2)\right] sds. \tag{26}$$

The remainder term R is now quadratic in E_u and will be neglected hereafter, assuming that the discrete solution U_h is indeed a sufficiently close approximation of U.

3.3 Error estimation

At this point we have an estimate of the approximation error given by

$$\mathscr{J}(U) - J(U_h) \approx F(Z - Z_h|D_h) - A(U_h; Z - Z_h|D_h), \tag{27}$$

where we have substituted Φ_h' by the adjoint solution of the discrete problem in Eq. (25), as usual in a posteriori error methodology. To be used, one needs to know the solution of the primal and dual discrete problems and of the continuous dual problem given by Eq. (10). However, the continuous dual problem can not be solved as it would require the knowledge of the exact solution U. Instead, a surrogate of Z denoted $\widetilde{Z}$ is used by solving a discrete dual problem on refined finite dimensional space $V_{\widetilde{h}}$ containing V_h.

The methodology is thus the following. Given an approximation space V_h we solve the primal and dual problems Eqs. (13,12) for U_h and $Z_h \in V_h$. To construct the refined space

$V_{\widetilde{h}} \supset V_h$, we increase the polynomial orders of both the approximation spaces of V_x and V_ξ, and we solve the following dual problem for $\widetilde{Z} \in V_{\widetilde{h}}$

$$\mathscr{J}'(U_h;\Phi') - A'(U_h;\Phi,\widetilde{Z}|D_{\widetilde{h}}) = 0, \quad \forall \Phi \in V_{\widetilde{h}}. \tag{28}$$

Two important remarks are necessary at this point. First, it should be underlined that dual problems are linear and usually much less costly to solve than the primal problems, even in an enriched approximation space using higher order polynomial approximations. Second, as shown by Eq. (28), the adjoint solution $\widetilde{Z}$ is based on functional form A' constructed with the approximation of D on the enriched space $V_{\widetilde{h}}$. As a consequence, the error estimate based on $\widetilde{Z}$ accounts for possible error in the approximation of the random parameters on V_h. When Eq.(28) is solved, the error estimate is

$$\mathscr{J}(U) - J(U_h) \approx F(\widetilde{Z} - Z_h|D_h) - A(U_h;\widetilde{Z} - Z_h|D_h), \tag{29}$$

4 DISCRETIZATION AND REFINEMENT

4.1 Stochastic discretization

The support of ξ is divided into a collection of N_b non-overlapping sub-domains, named blocks, $\Omega_\xi^{(l)}$ for $l = 1,\ldots,N_b$. These sub-domains are hyper-rectangles of Ω_ξ :

$$\Omega_\xi = \bigcup_{l=1}^{N_b} \Omega_\xi^{(l)}, \quad \Omega_\xi^{(l)} = [\xi_1^-,\xi_1^+] \times \cdots \times [\xi_n^-,\xi_n^+]. \tag{30}$$

On a sub-domain $\Omega_\xi^{(l)}$, the dependence of the solution with the random variables ξ is expanded on a set of orthogonal random polynomials $\Psi_k^{(l)}(\xi)$,

$$U(\xi \in \Omega_\xi^{(l)}) = \sum_{k=0}^{P(l)} u_k \Psi_k^{(l)}(\xi), \tag{31}$$

where the orthogonality is defined with regard to the "local" expectation (block-average) :

$$\left\langle \Psi_k^{(l)} \Psi_{k'}^{(l)} \right\rangle_{\Omega_\xi^{(l)}} = \int_{\Omega_\xi^{(l)}} \Psi_k^{(l)}(\xi)\Psi_{k'}^{(l)}(\xi) p_\xi(\xi) d\xi = \delta_{kk'} \left\langle {\Psi_k^{(l)}}^2 \right\rangle_{\Omega_\xi^{(l)}}. \tag{32}$$

The number of terms $P(l)$ in the expansion of Eq. (31) is function of the selected stochastic expansion order $q(l)$ of the block :

$$P(l) + 1 = \frac{(q(l)+n)!}{q(l)!n!}. \tag{33}$$

If the ξ_i are uniformly distributed over $\Omega_\xi^{(l)}$, then the polynomials $\Psi_k^{(l)}$ are simply rescaled version of the multidimensional Legendre polynomials. The refinement of the approximation of the solution can thus be improved by increasing the number of sub-domains, *i.e.* by splitting blocks into smaller ones, and/or by increasing the expansion order $q(l)$ over some given blocks.

4.2 Spatial discretization

Consider a partition of Ω_x into a set of N_x non-overlapping finite element with respective supports $\Omega_x^{(l)}$ for $l = 1, \ldots, N_x$:

$$\Omega_x = \bigcup_{l=1}^{N_x} \Omega_x^{(l)}. \tag{34}$$

For each element, the solution U_h is approximated by

$$U_h(x \in \Omega_x^{(l)}, \xi) = \sum_{i=1}^{Nd(l)} U_i^{(l)}(\xi) \mathcal{N}_i^{(l)}(x), \tag{35}$$

where $Nd(l)$ is the number of degrees of freedom of the l-th element and $\mathcal{N}_i^{(l)}$ the associated deterministic shape functions. We denote $p(l)$ the polynomial order of the shape functions over $\Omega_x^{(l)}$. The spatial approximation can be improved through h-refinement of the partition, *i.e.* by splitting elements, or through p-refinement consisting in increasing the polynomial order $p(l)$ of the approximation over one or more elements, *i.e.* by increasing the number of degrees of freedom of an spatial finite element.

4.3 Approximation space

With the stochastic and spatial discretization defined above and the tensorial form of the approximation space V_h,

$$V_h = \text{span}\{\mathcal{N}_i^{(l)}, 1 \leq i \leq N_d(l), 1 \leq l \leq N_x\} \times \{\Psi_k^{(m)}, 0 \leq k \leq P(m), 1 \leq m \leq N_b\}$$

the random solution at a point of $\Omega = \Omega_x \times \Omega_\xi$ writes as

$$U(x \in \Omega_x^{(l)}, \xi \in \Omega_\xi^{(m)}) = \sum_{i=1}^{Nd(l)} \sum_{k=0}^{P(m)} u_{i,k}^{(l,m)} \mathcal{N}_i^{(l)}(x) \Psi_k^{(m)}(\xi), \tag{36}$$

where deterministic coefficient $u_{i,k}^{(l,m)}$ is the k-th uncertainty mode of the i-th degree of freedom of the l-th element over the m-th probability block. A direct consequence of the tensored construction of the approximation space V_h is that the spatial mesh is the same for every probability blocks, and conversely the partition of Ω_ξ is the same for all spatial finite elements. This is clearly not optimal as some areas of the parameter domain Ω_ξ may require finer spatial discretization than others, while the solution in some parts of the spatial domain Ω_x may have complex dependences with $D(\xi)$, requiring a finer stochastic discretization than at other parts. The adaptation of the spatial discretization, *i.e.* the numbers of spatial elements N_x and of degrees of freedom per element N_d, over each sub-domain $\Omega_\xi^{(m)}$ is straight-forward, as the solution over different probability blocks

are fully independent with no differential operators along the uncertainty dimensions as a result. Such adaptation of the spatial mesh with probability blocks is in fact implemented in the solver used for the results presented hereafter. On the contrary, variable partition of Ω_ξ and stochastic expansion order for different spatial finite elements is much more cumbersome and remains to be investigated.

4.4 Refinement procedure

The a posteriori error methodology described in section 3 requires the resolution of the discretized primal and dual problems on V_h, followed by the resolution of a approximated dual problem on a enriched space $V_{\tilde{h}}$. The enriched space is constructed by increasing $p(l)$ the finite element order and $q(m)$ the stochastic expansion order. It gives access to an estimate of $\mathscr{J}(U) - \mathscr{J}(U_h)$ and we denote $\eta_{l,m}$ the estimate of the error over the m-th probability block and l-th spatial element and η the global error :

$$\eta_{l,m}^2 = \int_{\Omega_x^{(l)}} \int_{\Omega_\xi^{(m)}} \|\mathscr{J}(u) - \mathscr{J}(U_h)\|^2 p_\xi(\xi) d\xi dx, \quad \eta^2 = \sum_{l=1}^{N_x} \sum_{m=1}^{N_b} \eta_{l,m}^2. \tag{37}$$

One popular strategy is to rearrange and refine the discretization in order to distribute the global error η uniformly over the stochastic elements $\Omega_x^{(l)} \times \Omega_\xi^{(m)}$, *i.e.* aiming at :

$$\eta_{l,m}^2 \simeq \frac{\eta^2}{N_x \times N_b} \qquad \forall l \in [1, N_x],\ \forall m \in [1, N_b]. \tag{38}$$

To this end, we considered that if $\eta_{l,m}$ is greater than a prescribed tolerance criteria then the stochastic elements $\Omega_x^{(l)} \times \Omega_\xi^{(m)}$ needs refinement. However, the a posteriori error estimate provides no information regarding the structure of the error or its respective possible contributions, so that it is not possible to decide whether a h (improved partition) or p (improved approximation order) refinement strategy should be used, and along which spatial and/or stochastic directions. Brutal strategies, such a an homogeneous splitting of $\Omega_x^{(l)}$ and $\Omega_\xi^{(m)}$ along all their respective dimensions is not an option in uncertainty quantification where the stochastic dimension n can be large, and a **directional** error analysis is required. We have derived such anisotropic error estimations on the basis of the works of Almeida *et al.* (2000)[15] and Feijóo *et al.* (2002)[16] for deterministic problems. The anisotropic error estimator, that will be detailed elsewhere, makes use of Clément interpolants to construct the recovered symmetric Hessian of the approximation, whose eigen-values and eigen-vectors characterized the principal directions of the error (see Peraire *et al.*, 1992[17]). Using theses error indicators it can be decided to split a stochastic element along one or multiple spatial or stochastic directions.

5 APPLICATION EXAMPLE

5.1 Uncertain Burgers equation

To test the a posteriori error estimator, we consider the 1-D Burgers equation on the domain $\Omega_x \in [x^-, x^+]$:

$$\begin{cases} \frac{1}{2}\left(U\left(1-U\right)\right)_x - \mu\, U_{xx} = 0, \quad \forall x \in [x^-, x^+], \\ U(x^-) = a, \quad U(x^+) = b. \end{cases} \tag{39}$$

Here, the uncertainty is assumed to be on the value of the viscosity only. It is expanded using two random variables $\xi = \{\xi_1, \xi_2\}$ with uniform distribution on $[-1, 1]$:

$$\mu(\xi) = \mu_0 + \mu_1\xi_1 + \mu_2\xi_2, \quad \mu_1, \mu_2 > 0 \tag{40}$$

For this settings, the mean viscosity is μ_0 and the range of μ is $[\mu_0-(\mu_1+\mu_2), \mu_0+(\mu_1+\mu_2)]$. Then, for the problem to be well-posed we must have $\mu_1 + \mu_2 < \mu$.

Equations of the dual problem are

$$\begin{cases} \frac{1}{2}\, Z_x - U\, Z_x + \mu\, Z_{xx} = 1, \quad \forall x \in [x^-, x^+], \\ Z(x^-) = 0, \quad Z(x^+) = 0. \end{cases} \tag{41}$$

The primal and dual problems are solved with Chebyshev finite elements in space and 2-dimensional rescaled Legendre polynomials (uniform density) along the stochastic dimensions[18].

5.2 Results

Unless otherwise stated, the viscosity parameters adopted throughout the paper are $\mu_0 = 1$, $\mu_1 = 0.82$ and $\mu_2 = 0.16$ and the spatial domain is defined by $x^- = -10$, $x^+ = 10$. The probability density function (*pdf*) of μ is plotted in figure 1 where it can be noted that the viscosity is never null or negative as $P(\mu < 0.02) = 0$ thus ensuring that the problem is well-posed.

Figure 2 shows the first (left) and second (right) statistical moments of the solution. The mean solution $\langle u(x,\xi)\rangle = u_0(x)$ is seen to exhibit a hyperbolic tangent-like profile but is clearly different from the solution corresponding to a mean value of the viscosity $\mu = 1$. This is due to the non-linear character of the problem, introducing a bias between the mean solution and the solution for the mean parameters. On the right, the variance $\sigma^2(u)$ is plotted. The boundary conditions are deterministic and the variance of u is thus zero at these locations. The uncertain character of the viscosity does not introduce any asymmetry in the problem and, as $x^- = x^+$, it follows that $u(x = 0 \mid \mu) = 1/2$ almost surely and $\sigma^2(u(x = 0 \mid \mu)) = 0$.

The probability density function of the solution is plotted in figure 3 (left). In addition to the null variance at the boundary and $x = 0$ (at those points, the *pdf* is a dirac

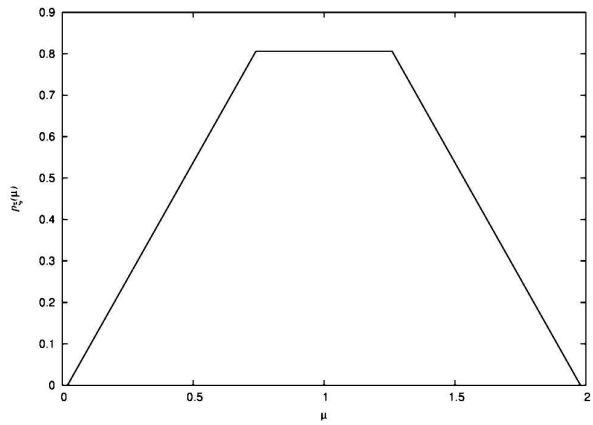

Figure 1: Probability density function of the viscosity.

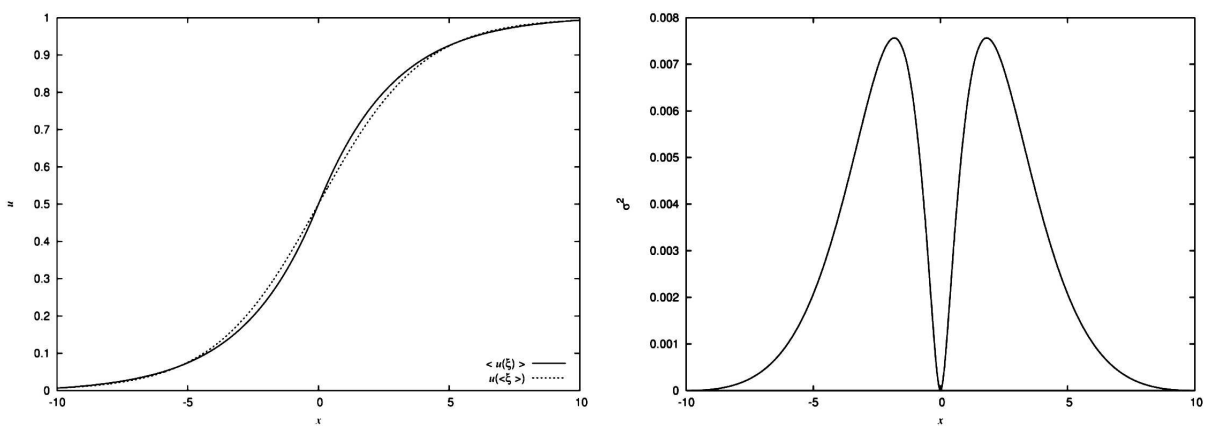

Figure 2: First statistical moments of the solution. Mean (left) and variance (right).

function), it can be seen that the *pdf* changes a lot along the x-direction, evolving from a dirac at the left boundary condition to a highly asymmetric pattern for moderate negative x and to a dirac again at $x = 0$. Thanks to the symmetry of the problem, the *pdf* is also symmetric about the point $x = 0$. The high asymmetry in the tails of the *pdfs* at a particular x and its quickly evolving nature along x motivates the need for an efficient way of accounting for the uncertainty in the solution. A global Polynomial Chaos formulation over Ω_ξ would require a prohibitively large number of terms to approximate such a steep solution and the solution process would most likely not even converge. The spectral elements approach in the stochastic space is thus fully justified here.

The asymmetric character of the *pdf* at a particular location in x can also be appreciated from figure 3 (right) which shows the quantiles of the solution. The plotted quantiles correspond to the cumulated probability $\{0.05, 0.15, \ldots, 0.85, 0.95\}$ of cumulated probability. While they represent solutions that are uniformly spaced in the [0; 1] range of

cumulated probability, their spatial distribution is seen to be non-uniformly spaced between the two extreme quantiles 0.05 and 0.95, revealing a non-symmetric *pdf*.

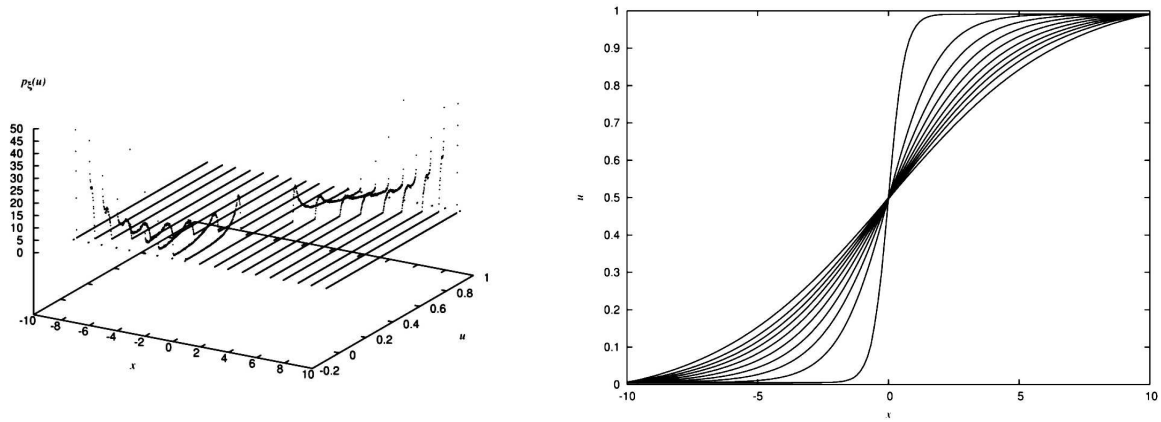

Figure 3: Left: Probability density function of the solution. The *pdf*-axis scale is truncated for clarity. Right: Quantiles of the solution $\in \{0.05, 0.15, \ldots, 0.85, 0.95\}$

The solution being steep, some elements need refinement. To investigate how the solution accuracy improves as the refinement process goes, the plot in figure 4 shows the local *pdf* at $x = 0.52$ for different stages of the refinement process. To enhance the difference between the plots, the *pdf* is here plotted using a logarithmic scale. As the refinement goes, referenced with the iteration number, the solution is seen to exist on a wider support, having a much longer tail. The far tail corresponds to solutions affected with a very low probability. Accurately determining these rare solutions is usually difficult as it requires a very large number of terms (PC method) or samples (MonteCarlo technique). Here, the derived method allows for a good representation with a limited number of terms as the *pdf* converges in about 4 to 5 iterations only.

Examining the resulting mesh in the ξ-subspace, figure 5 (left), the refinement is seen to most affect the lower left corner, corresponding to low ξ_1 and ξ_2. Recalling the viscosity expresses as $\mu(\xi) = \mu_0 + \mu_1\xi_1 + \mu_2\xi_2$, with $\mu_i > 0\ \forall i \in \{0, 1, 2\}$, the lower left corner corresponds to lowest values of the viscosity. As the solution behaves as $u(x, \mu) \sim \tanh(x/\mu)$, the steepness of the solution depends on the viscosity with a low viscosity corresponding to a sharp solution. The refinement process thus consistently adds some information in regions corresponding to the most "difficult" local problems.

The resulting mesh in the $\Omega_x \times \Omega_\xi$ space is represented in figure 5 (right). In addition to the refinement in the ξ-subspace, the x-subspace is seen to be refined as well, in particular around $x = 0$. This again corresponds to the region of solution where the steepness of the problem is the largest and thus requires the finest discretization. It can also be noted that the x-refinement depends on the value of the viscosity as for positive ξ_i, corresponding to large viscosity, the x-grid is coarse due to a smoother solution.

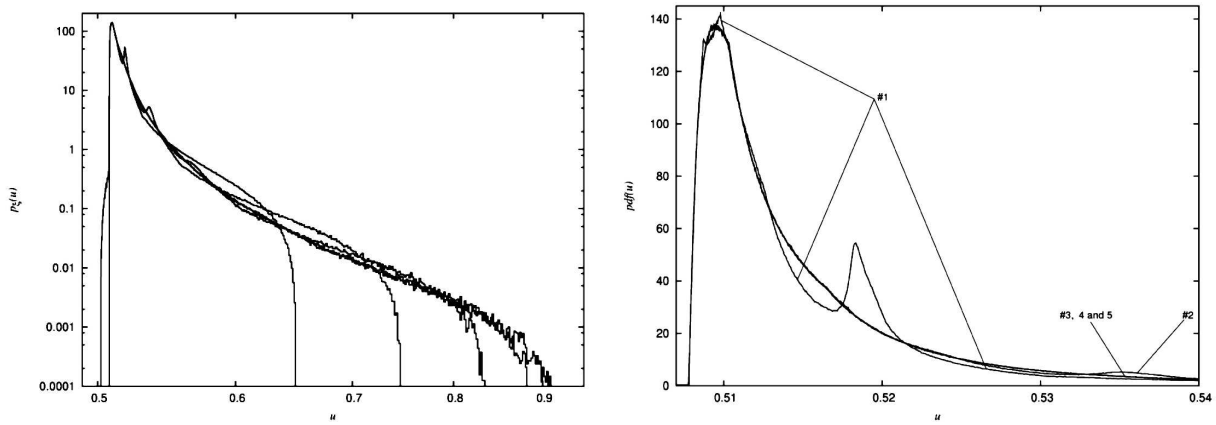

Figure 4: Probability density function at $x = 0.52$ for different steps of the refinement process. General log plot (left) and zoom (right).

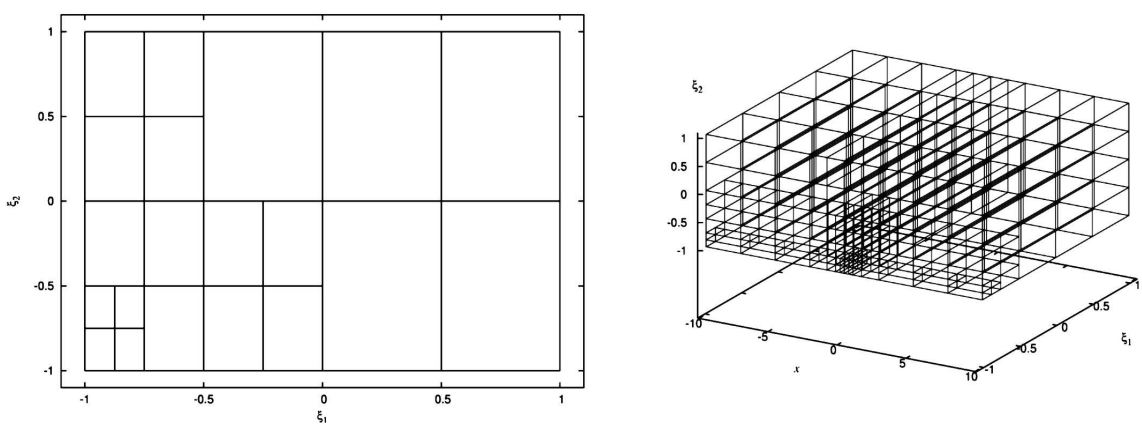

Figure 5: Stochastic (left) and spatial-stochastic (right) space partitioning after the refinement procedure.

The different stages of the refinement process on the solution space partition can be seen in figure 6 where the surface response of the solution at $x = 0.52$ together with the mesh in the $\{x; \xi\}$-space are plotted for different iterations. Starting with a coarse initial mesh, both in the spatial and stochastic domain at iteration #1, one can note that the refinement in the ξ-space occurred only along the ξ_1 dimension. This is due to the largest steepness of the problem along that particular dimension (recall we have $\xi_1 > \xi_2$). At iteration #3, the mesh is seen to be further refined in the region of largest steepness, around $x = 0$ and for low ξ_i. At iteration #4, the solution is converged in the sense of the accuracy prescribed for that particular case. The block corresponding to the lowest ξ_i is the only one to have been further refined from iteration #3.

The convergence of the refining process may be appreciated from figure 7 showing the evolution of the relative error as the number of elements is increased from 2 to 99 in each of the two stochastic dimensions ξ_1 and ξ_2, the polynomial order q of the Polynomial

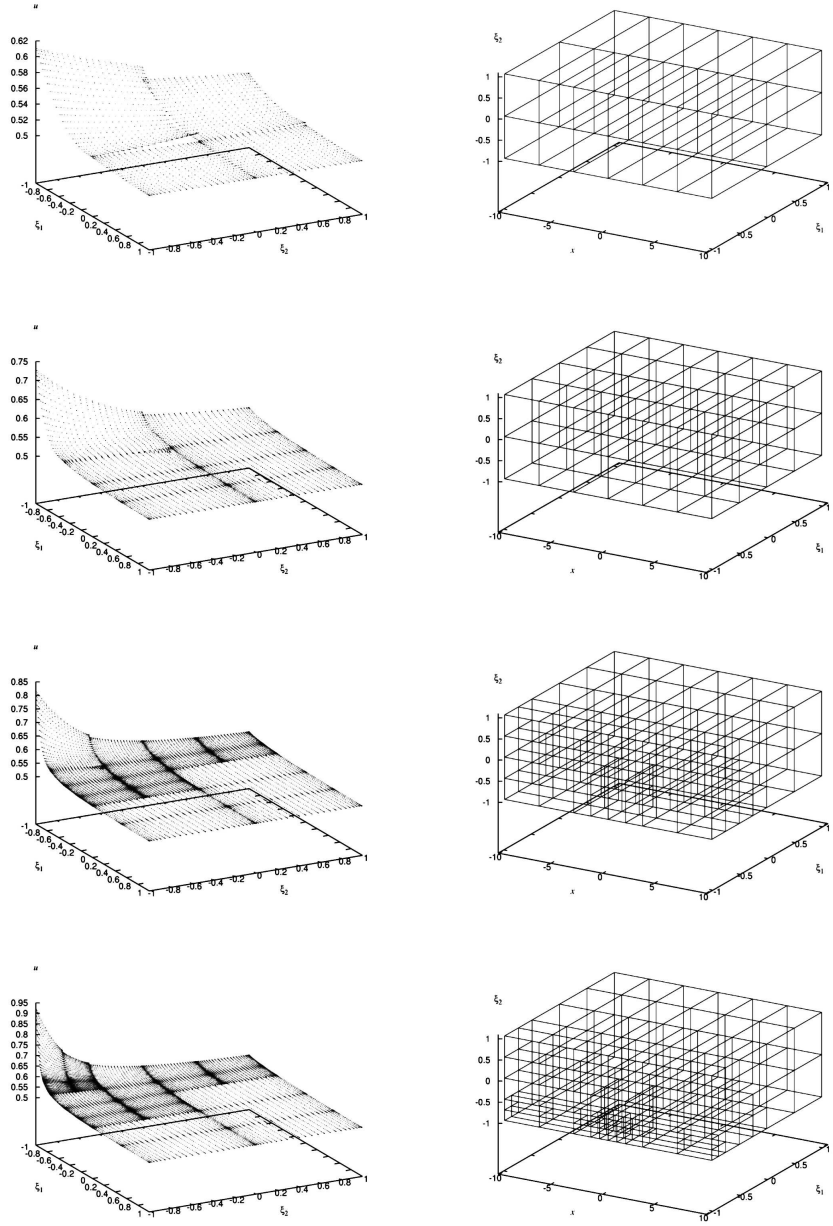

Figure 6: Surface response along 4 refinement iterations.

Chaos development remaining constant, figure 7 (left). The n-dimensional blocks, defined by the elements along each ξ_i dimensions, are paving the stochastic space and their total number $N_{b,tot}$ varies from 4 to 9801. The convergence is investigated for the mean solution and its variance at the particular location $x = 0.52$ where the solution has already been seen to be steep. Two different polynomial orders were used, $q = 2$ and $q = 4$. The error

is seen to quickly decrease as the number of blocks increases, illustrating the convergence of the solution process. The error on both the mean and the variance converges with a similar rate.

In figure 8, the relative error evolution is plotted along the refinement process. It is seen to dramatically speed-up the convergence, allowing to reach an error similar to the one obtained using $N_{b,tot} \simeq 5000$ but for only $N_{b,tot} = 128$. To make a fair comparison between the a priori set mesh partition and the partition generated through the a posteriori analysis process, the error in the mean and the variance of the solution is plotted as a function of the total number of elementary computations required. Indeed, the refinement procedure split some elements in smaller blocks and the solution of the problem is then solved on each of these new blocks, even if the solution on the preceding larger block was already computed. It is necessary to account for those discarded computations to accurately compare the convergence performance in terms of required overall computational load.

The whole refinement process steps are given in table 1.

Iteration #	# of blocks	Cumulated # of blocks	ε_{mean}	$\varepsilon_{variance}$
1	4	4	$4.1074\ 10^{-5}$	$1.0189\ 10^{-3}$
2	16	20	$4.7861\ 10^{-5}$	$2.7054\ 10^{-3}$
3	64	84	$1.0813\ 10^{-5}$	$7.1067\ 10^{-4}$
4	76	100	$1.3056\ 10^{-6}$	$1.0944\ 10^{-4}$
5	88	116	$8.7892\ 10^{-8}$	$8.5915\ 10^{-6}$
6	97	128	$6.9087\ 10^{-9}$	$1.4032\ 10^{-7}$

Table 1: Convergence of the refinement process.

Starting from a 4-block initial stochastic space partition, all blocks are found to require refinement at the first iteration, leading to a 16-block partition. At the next iteration, all these newly created subdomains are still considered too coarse to match the prescribed accuracy and all are refined, resulting in a 64-block partition. At this step, only a few blocks need further refinement and the process eventually stops after 6 iterations with a 97-blocks partitioning of the stochastic space. The total number (cumulated) of solvings of the problem is 128, much less than the 5000-block partition required in the uniform mesh approach to reach the same accuracy.

The influence of the local Polynomial Chaos order q in the elements is seen in figure 9 where the space partitioning resulting from the refinement process is shown when different polynomial orders are considered. As expected, the stochastic space requires a strong refinement when q is low to reach the prescribed accuracy (top) while a few blocks suffice when $q = 5$ (bottom).

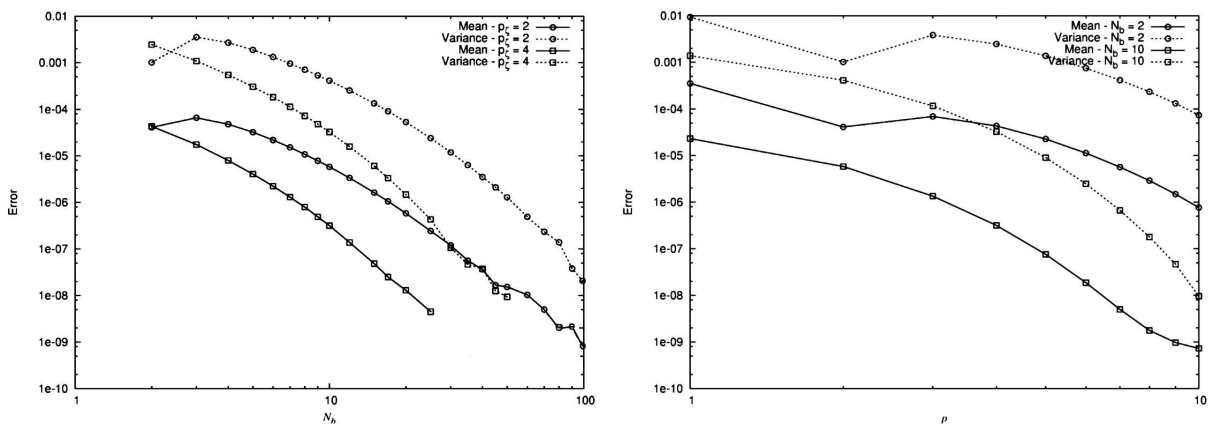

Figure 7: Error convergence with a finer discretization. h-convergence (left) and p-convergence (right).

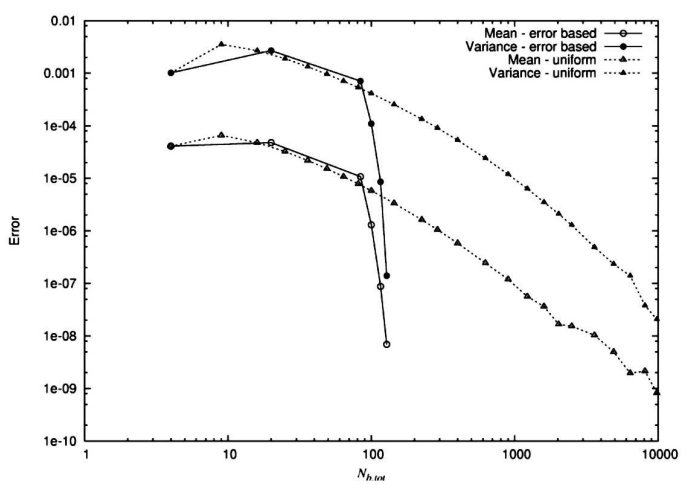

Figure 8: Comparison of the error with the total (cumulated) number of blocks in the stochastic space.

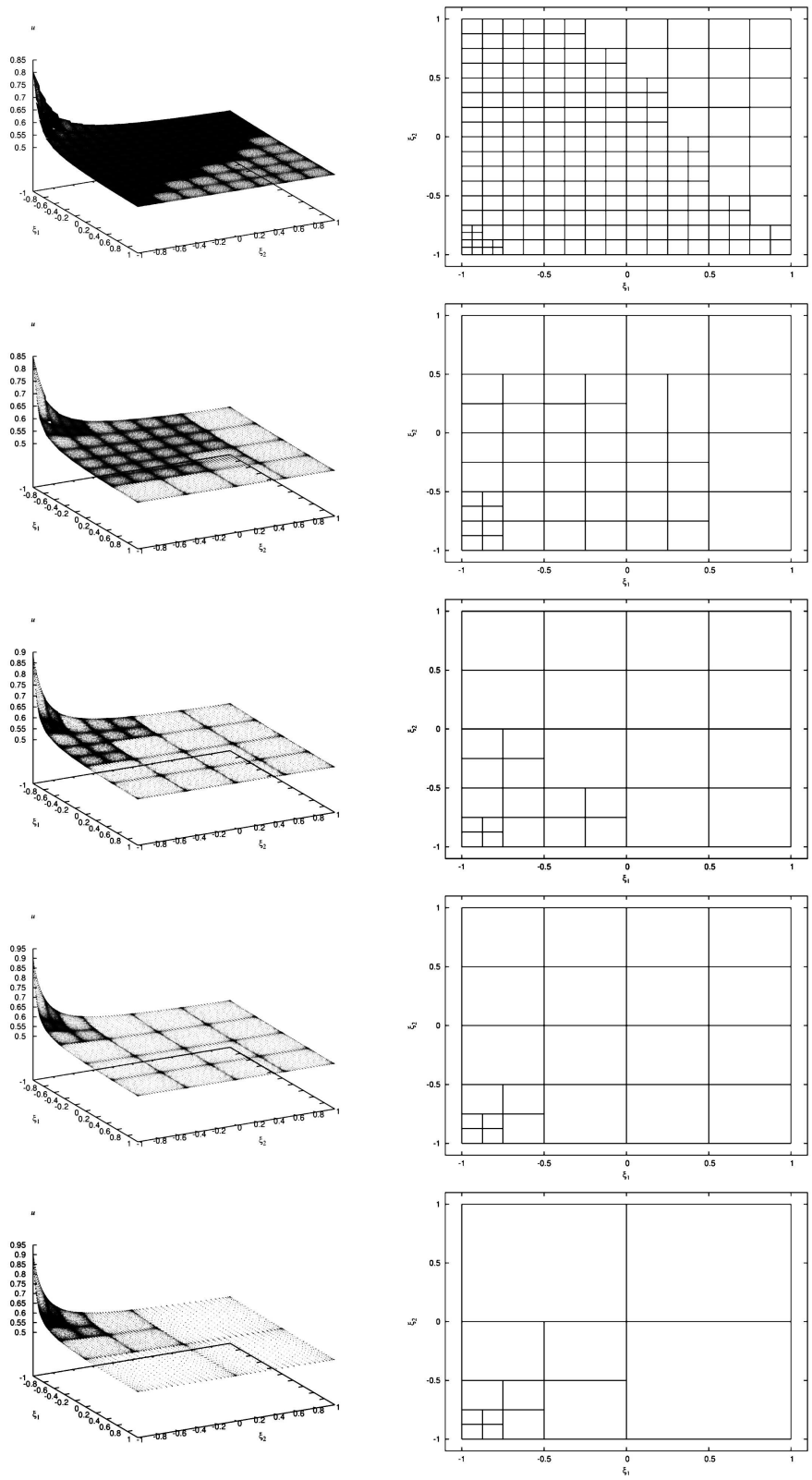

Figure 9: Increasing the initial Polynomial Chaos order at constant accuracy tolerance. From top to bottom, $q = 1$ to 5.

6 CONCLUDING REMARKS

Techniques to quantify and propagate uncertainty in the numerical simulations has recently been developed and, in particular, the Polynomial Chaos decomposition was proved effective. However, no rigorous criterion was available to quantify the degree of approximation of the solution by this decomposition. This paper aims to be a contribution to that issue in deriving a dual-based a posteriori error analysis of an uncertain test problem. This approach allowed to propose an algorithm to refine the discretization of the uncertain problem only where the estimated error is larger than a preset tolerance. In case of a hp-stochastic formulation for the discretization, it was shown that the element diameter and/or the polynomial order can be modified to improve the accuracy of the solution (h/p-refinement), while keeping the total number of degrees of freedom low. Examples based on the uncertain Burgers equation have shown how effective and flexible this approach may be.

References

[1] N. Wiener, The homogeneous chaos, *Amer. J. Math.*, **60**(4), 897–936, (1938).

[2] O.P. Le Maître, O.M. Knio, H.N. Najm and R.G. Ghanem, A stochastic projection method for fluid flow. I. Basic formulation, *J. Comput. Phys.*, **173**(2), 481–511, (2001).

[3] O.P. Le Maître, M.T. Reagan, O.M. Knio, H.N. Najm and R.G. Ghanem, A stochastic projection method for fluid flow. II. Random process, *J. Comput. Phys.*, **181**(1), 9–44, (2002).

[4] B. Debusschere, H.M. Najm, A. Matta, O.M. Knio, R.G. Ghanem and O.P. Le Maître, Protein labelling reactions in electrochemical flow: numerical simulation and uncertainty propagation, *Phys. Fluids*, **15**(8), 2238–2250, (2003).

[5] L. Mathelin, M.Y. Hussaini and T.A. Zang, Stochastic approaches to uncertainty quantification in CFD simulations, *Num Algo.*, **38**(1), 209–239, (2005).

[6] D.B. Xiu and G.E. Karniadakis, The Wiener-Askey polynomial chaos for stochastic differential equations, *SIAM J. Sci. Comput.*, **24**(2), 619–644, (2002).

[7] D.B. Xiu and G.E. Karniadakis, Modeling uncertainty in flow simulations via generalized polynomial chaos, *J. Comput. Phys.*, **187**, 137–167, (2003).

[8] O.P. Le Maître, H.N. Najm, R.G. Ghanem and O.M. Knio, Multi-resolution analysis of Wiener-type uncertainty propagation schemes, *J. Comput. Phys.*, **197**(2), 502–531, (2004).

[9] X. Wan and G.E. Karniadakis, An adaptive multi-element generalized polynomial chaos method for stochastic differential equations, *J. Comput. Phys.*, **209**, 617–642, (2005).

[10] R.G. Ghanem and P.D. Spanos, *Stochastic finite elements. A spectral approach*, Dover Publications, Inc., 222 p., (1991).

[11] B.V. Asokan and N. Zabaras, Using stochastic analysis to capture unstable equilibrium in natural convection, *J. Comput. Phys.*, **208**, 134–153, (2005).

[12] I. Babuška and W.C. Rheinboldt, A posteriori error estimates for the finite element method, *Int. J. Numer. Meth. Engrg.*, **12**, 1597–1615, (1978).

[13] I. Babuška and A.D. Miller, A feedback finite element method with a posteriori error estimation, *Comput. Methods Appl. Mech. Engrg.*, **61**, 1–40, (1987).

[14] R. Becker and R. Rannacher, An optimal control approach to a posteriori error estimation in finite element methods, *Acta Numer.*, **10**, 1–102, (2001).

[15] R.C. Almeida, R. A. Feijóo, A.C. Galeão, C. Padra and R.S. Silva, Adaptive finite element computational fluid dynamics using an anisotropic error estimator, *Comput. Methods Appl. Mech. Engrg.*, **182**, 379–400, (2000).

[16] R.A. Feijóo, C. Padra and F. Quintana, An anisotropic a posteriori error estimator for CFD, *Int. J. Comput. Fluid Dyn.*, **16**(4), 297–304, (2002).

[17] J. Peraire, J. Peiró and K. Morgan, Adaptive remeshing for three-dimensional compressible flow computations, *J. Comput. Phys.*, **103**(2), 269–285, (1992).

[18] M. Abramowitz and I. Stegun, *Handbook of mathematical functions*, Dover, (1970).